Electromagnetic Thermal Coupled Analysis of a Linear Induction Furnace with Rotational Symmetry

Asst. Prof. Dr. Akram F. Batti
Educational Technology Department
University of Technology, Baghdad, Iraq

Asst. Prof. Dr. Abdul-Karim Z. Mansur
Electrical Department
Technical College, Mosul, Iraq

Dr. Fadhil A. Abood
Educational Technology Department
University of Technology, Baghdad, Iraq

Lect. Essam M. Abdul-Baki
Electrical Eng. Dept., Al-Rasheed College
University of Technology, Baghdad, Iraq

Abstract

This research deals with a modeling of the heating process of an induction furnace with a conducting non-ferromagnetic core. This is done by performing a sequential coupling between two types of analysis; the harmonic electromagnetic analysis and the transient thermal analysis in order to furnish a complete numerical simulation of this device.

The Finite Element Method (FEM) is considered in order to solve this problem using the "ANSYS" computer package. The proposed coupling algorithm deals with different heat treatment procedures by induction for any axi-symmetrical linear work piece has been built. The obtained results show a good agreement with the published practical measurements.

This work aids to declare the behavior of the furnace during the heating process, and leads the designer to determine the required geometry of the furnace, its excitation current and frequency suitable to do certain heat treatment of a defined work piece in shape and composition. So, this algorithm is a computer aided design for a linear induction furnace with rotational symmetry. This algorithm can be used to design such devices instead of the traditional trial and error, experience dependant, design methods which lead to loss time, money and efforts.

الخـــلاصـــــــة

يهتم البحث بنمذجة عملية التسخين بفرن حثي ذو قلب من مادة لامغناطيسيه موصله.لقد تم ذلك بأجراء تعشيق متتالي بين نوعين من التحليلآت؛ التحليلآت الكهرومغناطيسيه التوافقيه و التحليلآت الحراريه العابره وذلك لغرض الحصول على نمذجه رقميه كامله لهذا الجهاز.

أعتمدت طريقة طريقة العنصر المحدد(FEM) لحل هذه المعضله باستخدام برامجيات الحاسبه الألكترونيه (ANSYS). ان الخوارزميه المقترحه تعنى بمختلف سياقات المعاملات الحراريه الحثيه للعينات الخطيه المتناضره محوريا. بينت النتائج المستحصله أنسجاما جيدا مع القياسات العمليه المنشورة.

أن هذا العمل ساعد على توضيح طريقة تصرف الفرن خلال عملية التسخين وقيادة المصمم الى تحديد الشكل الهندسي المطلوب للفرن وتيار التحفيز و التردد المناسب لأجراء معامله حراريه معينه لعينه ذات شكل وماده محددين. لذا فأن الخوارزميه المقترحه هي عبارة عن تصميم بمساعدة الحاسبة لمثل هذه الاجهزة بديلا عن تلك الطرق التقليديه التي تعتمد الخبرة وأسلوب ألتجربة و الخطأ و التي تؤدي الى خسارة المال والوقت والجهود.

1. Introduction

It is already known that the induced eddy currents inside the induction furnace core (the work piece or the specimen) is not uniform, and it depends on many factors like, the frequency of the excitation current, the shapes of the furnace and the specimen to be heated, the electrical conductivity and relative permeability of the core material .

The mathematical simulation of a linear induction furnace is a complicated problem due to the non uniform distribution of the induced eddy currents inside its core which leads to a non uniform heat distribution. Since the physical properties throughout the core material vary with temperature, the real behavior of the core can be simulated during the heating period by dividing the core into very small parts. A harmonic electromagnetic analysis is done for each part alone to determine its induced eddy current losses. Then these values considered as input data to a transient thermal analysis step to study the heat transfer for the core for a short period of time and determine the temperature distribution inside the core at the end of that period. Hence to calculate the temperature distribution for the next short period of time the above procedure must be repeated after updating the properties due to the new temperature of each part and so on until the heating period is finished by reaching the specified temperature distribution inside the core.

This problem can be solved numerically by digital computer using the Finite Element Method (FEM). It starts by dividing the region under study into a finite elements and making the calculations in each element separately by considering its temperature and updating the values of its material properties due to that temperature. A finite element computer package ANSYS used for this purpose and a computer program is done to model this process. The modeling is done by make a sequential coupling between two different kinds of analysis, the steady state linear harmonic electromagnetic analysis and the transient thermal analysis. **Figure (1)** shows the block diagram of this algorithm.
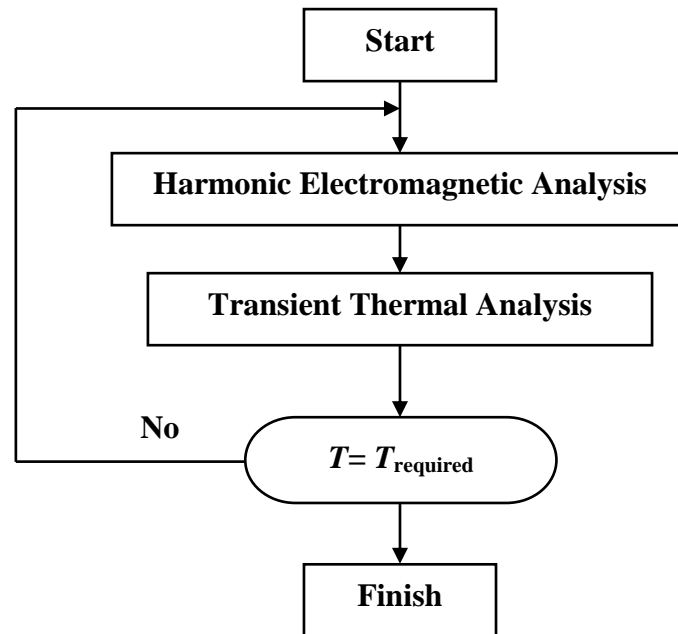
Figure (1) General block diagram of the algorithm

2. Theoretical Background

2-1 Electromagnetic Analysis

It is already known that the complex electromagnetic equations can be greatly simplified based on magnetic vector potential *A*. All quantities related to the induction Joule heat can be achieved, based on the current, I, input to the induction coil. *A* can be expressed with Biot-Savart's law [1].

$$\mathbf{A} = \frac{\mu_o \mathbf{I}}{4\pi} \int_s \frac{\mathbf{dl}}{|\mathbf{r}|} \quad \text{...} \quad (1)$$

The magnetic flux density *B* is defined as:

$$\mathbf{B} = \nabla \times \mathbf{A} \quad \text{...} \quad (2)$$

From Faraday's law, the electric field intensity *E* and magnetic field intensity *H* are related by the following equations:

$$\nabla \times \mathbf{E} = -\frac{\partial \mathbf{B}}{\partial \mathbf{t}} \quad \text{...} \quad (3)$$

$$\mathbf{H} = \mathbf{B}/\mu \quad \text{...} \quad (4)$$

Based on Ampere's circuital law, the current density, *J*, induced in work piece is:

$$\mathbf{J} = \nabla \times \mathbf{H} - \frac{\partial (\varepsilon \cdot \mathbf{E})}{\partial t} \dots\dots\dots\dots\dots\dots\dots\dots\dots\dots\dots\dots\dots\dots\dots \quad (5)$$

After a mathematical manipulations of the above formulas, the relationship between the magnetic vector potential, *A*, and the induced current density, *J*, becomes:

$$\mathbf{J} = \nabla \times (\frac{1}{\mu} \nabla \times \mathbf{A}) + \sigma_e \frac{\partial \mathbf{A}}{\partial t} \dots\dots\dots\dots\dots\dots\dots\dots\dots\dots\dots\dots\dots \quad (6)$$

Finally, Joule heat generated from eddy currents is:

$$\mathbf{Q}_{induction} = \frac{\mathbf{J}^2}{\sigma_e} \dots\dots\dots\dots\dots\dots\dots\dots\dots\dots\dots\dots\dots\dots\dots\dots\dots \quad (7)$$

where,

$\mu, \varepsilon, \sigma,$ *: are the magnetic permeability, permittivity, and electrical conductivity of the medium respectively. These properties are all temperature dependent, and this makes the electromagnetic analysis as a highly non-linear problem.*

2-2 Thermal Analysis

Thermal analysis includes conduction, convection and radiation. The heating process is coupled with the electromagnetic conversion process. In the heating process, the heat conduction effect is the main issue to be considered because the heating cycle is generally very short as several seconds. The conduction equation is [2]:

$$\rho_m \cdot C_p \cdot \frac{\partial \mathbf{T}}{\partial t} = k \cdot \nabla^2 \mathbf{T} + \mathbf{Q}_{induction} \dots\dots\dots\dots\dots\dots\dots\dots\dots\dots\dots \quad (8)$$

where:

$Q_{induction}$ *: is the Joule heat from the electromagnetic process, which is known as HGEN in ANSYS terminology.*

On surfaces of work piece, the heat conduction, radiation and free convection effects are all needed. The governing equation is:

$$\rho_m \cdot C_p \cdot \frac{\partial \mathbf{T}}{\partial t} = k \cdot \nabla^2 \mathbf{T} + \mathbf{Q}_{induction} - \xi \cdot \sigma_s \cdot (\mathbf{T}^4 - \mathbf{T}_{air}^4) - \alpha \cdot (\mathbf{T} - \mathbf{T}_{air}) \dots\dots\dots\dots \quad (9)$$

where:

T_{air}*: is the ambient temperature*

3. The Analysis

C. Chaboudez et. al. [3] presented a suitable induction heating practical measurements for a work piece of a conducting non-ferromagnetic material of stainless steel type X5CrNi 18/9 (1.4301). The orientation of the upper part of this work piece is placed inside a coil winding made of copper as shown in **Fig.(2)** and the geometric characteristics of the induction heating setup are shown in **Table (1)**. It should be mentioned that the coil starts (12.5 mm) above the work piece. The thermocouple used in this measurement was spark welded on the surface in order to ensure a good thermal contact at the location represented in **Fig.(2)**, the power supply of the furnace is a 10 kHz rotating converter, and the heating time is 25 s with current density of (50.78E+06) A.m^{-2}.
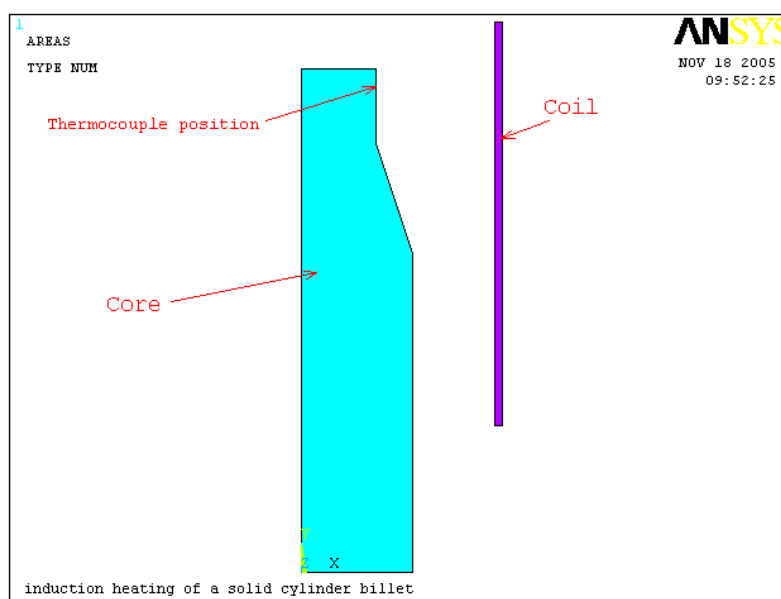
Figure (2) Stainless steel work piece and its position inside the furnace

Table (1) Dimensions of the furnace

Total length of the work piece	135 mm
Length of the lower cylindrical part	85 mm
Diameter of the lower cylindrical part	30 mm
Length of the upper cylindrical part	20 mm
Diameter of the upper cylindrical part	20 mm
Internal diameter of the coil	50 mm
External diameter of the coil	52 mm
Length of the coil	108mm
Distance from the top of the work piece to the thermocouple	5 mm

The magnetic permeability of the stainless steel μ is assumed to be $\mu_o = 4\pi \times 10^{-7}$. The conductivity σ (expressed in $\Omega^{-1}m^{-1}$) varies with the temperature T according to the formula [4]:

$$\sigma(T) = \frac{1}{a + bT + cT^2 + dT^3}$$ ……………..………………………………………. (10)

With a=4.9659E-07, b=8.4121E-10, c=-3.7264E-13, and d=6.1960E-17. **Figure (3)** shows the variation of the electrical resistivity $\left[\rho(T) = 1/\sigma(T)\right]$ of the core (work piece) with temperature.
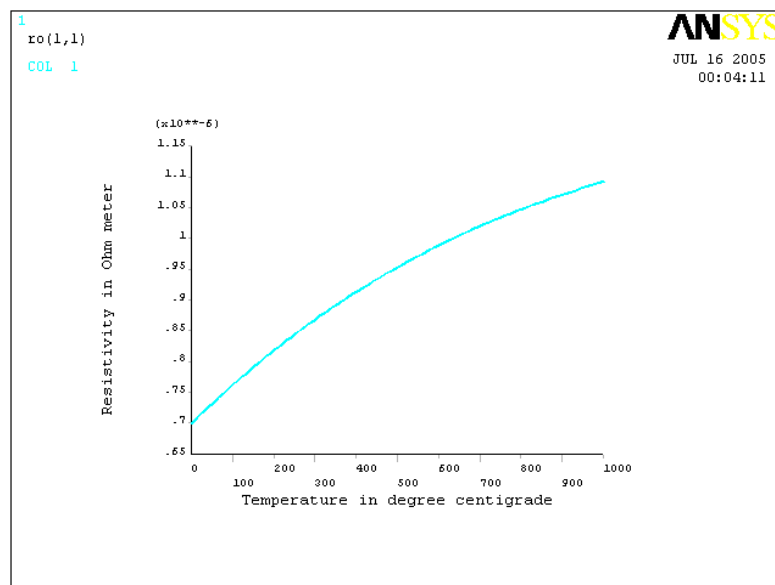
Figure (3) The variation of the electrical resistivity with temperature of a non-ferromagnetic stainless steel X5CrNi 18/9 (1.4301)

The thermal conductivity λ (in $Wm^{-1}K^{-1}$) of the core material is [4]:

$$\lambda(T) = 100(a + bT)$$ ………………...…..…………………………………… (11)

With a = 0.11215 and b = 1.4087E-04. [4]; **Fig.(4)** shows the variation of the thermal conductivity of the core with temperature.
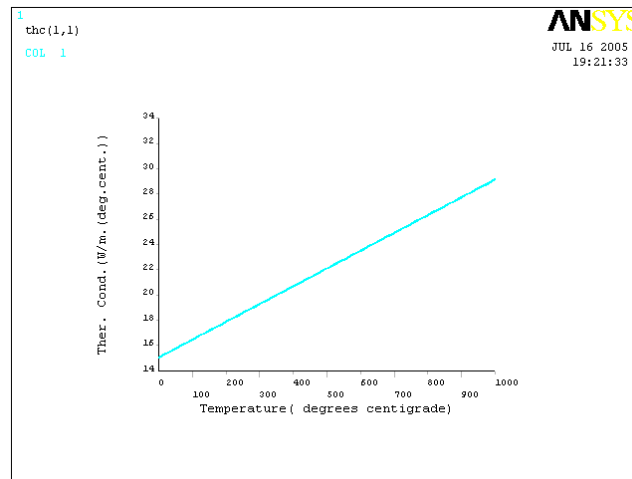
Figure (4) Variation of Thermal conductivity with temperature for non-ferromagnetic stainless steel X5CrNi 18/9 (1.4301)

And the volumic heat capacity ρC_p (in $JK^{-1}m^{-3}$) has the form [4]:

$$\rho C_p(T) = 7.9 \times 10^6 (a + bT) \quad .... (12)$$

With a = 3.562E-01 and b = 0.988E-04 [4]. In order to find the enthalpy (*Enth*) for this material

$$Enth = C_p(T) * T$$

Since ρ for steel is 7800 Kg m^{-3} then:

$$\textbf{Enth (T)} = (7.9 \times 10^6 (a + bT)\big/(7800)) \times T \quad .... (13)$$

Figure (5) shows the variation of the enthalpy of the core material with temperature.
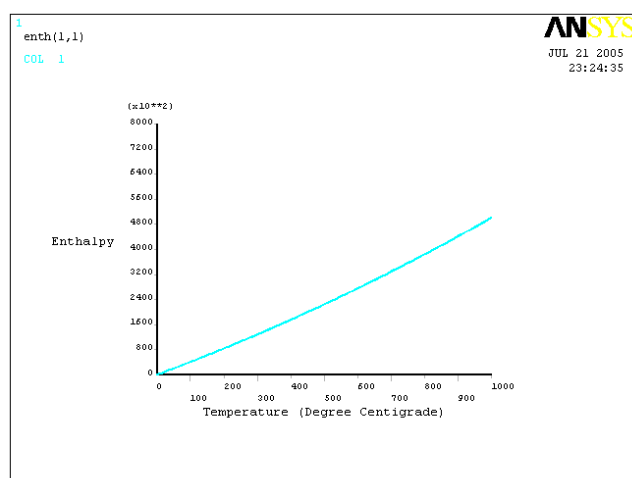
Figure (5) Shows the variation of the enthalpy with temperature of a non-ferromagnetic stainless steel X5CrNi 18/9 (1.4301)

4. The Furnace Simulation using FEM

The furnace simulation steps are shown in the detailed flowchart in **Fig.(6)**, in which step 1 is the formation of the system and meshing it.
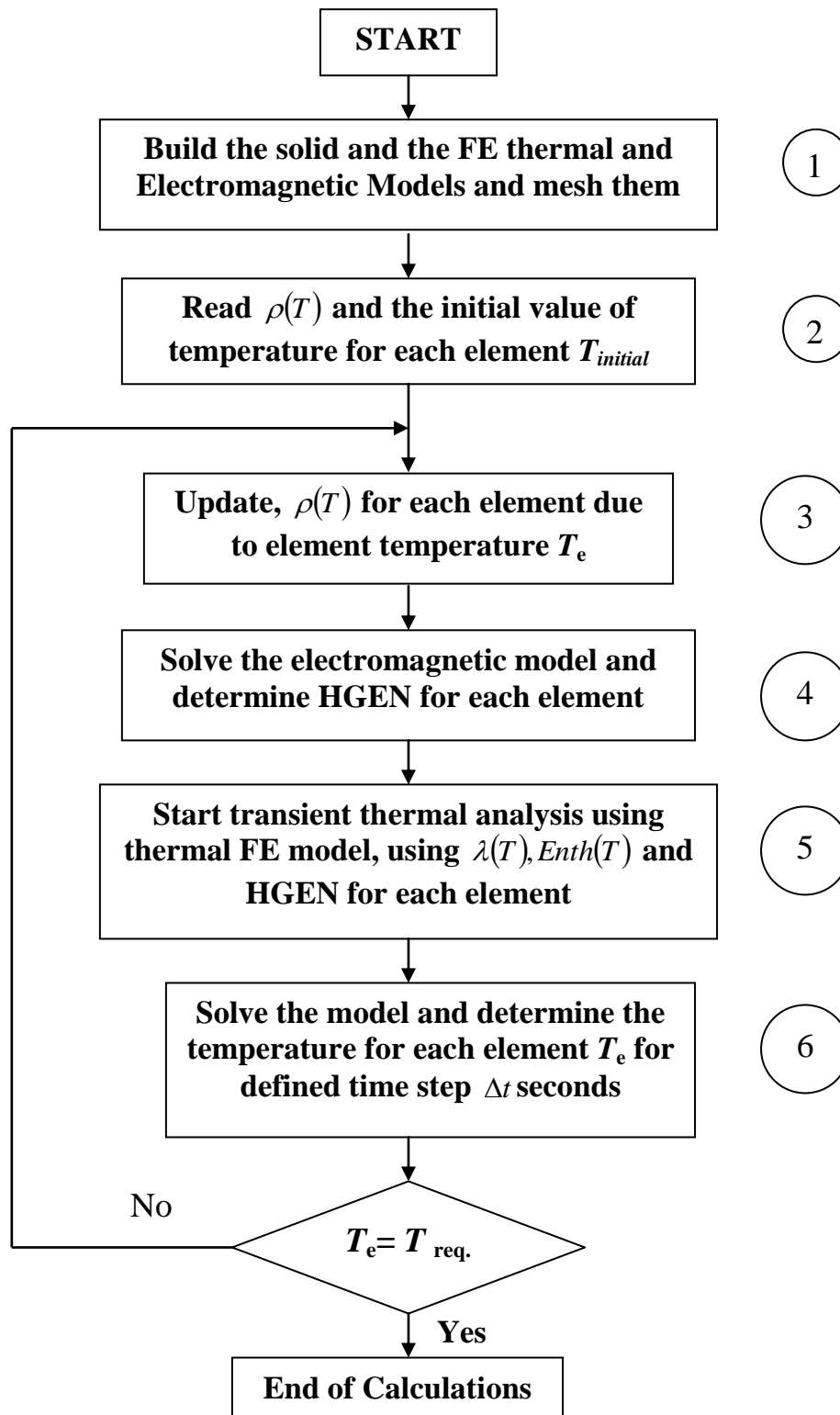

Figure (6) Flow chart for electromagnetic-thermal coupled analysis for ferromagnetic materials core

  Figs.(7), **(8)**, **(9)**, and **(10)** show these steps. **Figure (7)** shows the coil, the work piece and the boundary region areas. It is clear that the geometrical shape permit to use half axi-symmetry in this analysis. Also, it should be mentioned here that the original example uses a multi turns coil characterized in that the spacing betweens these turns is not constant, but it differ in order to achieve a uniform heat distribution at the work piece surface, and the coil conductor is a hollow rectangular conductor of dimensions $5 \times 10\,\text{mm}$ with wall thickness of 1mm in order to permit a cooling water to flow inside it. But in this analysis the coil is considered as a solid conducting copper plate of rectangular cross section $2 \times 108\,\text{mm}$ equivalent to the same cross-sectional area fed by a constant current density. The value of this current density is calculated to furnish the same current passing through the actual coil in the practical case. The mesh of the whole model will be as shown in **Fig.(8)**, which represents the surface elements deals with the heat radiation from the work piece. In steps 2 and 3 the program reads the function $\rho(T)$ and determines the resistivity of each element due to the initial temperature assumed.
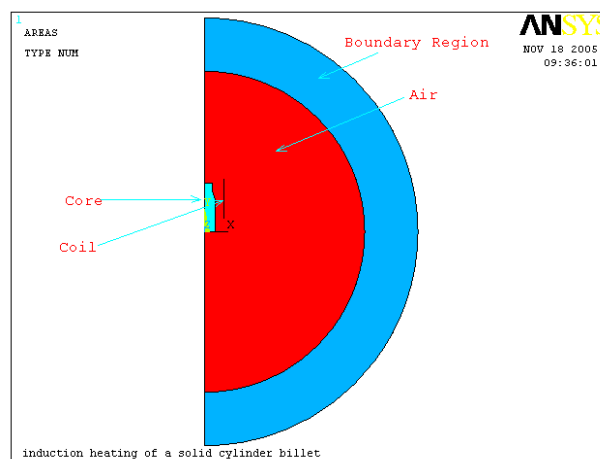

**Figure (7) Represents the orientation of the induction furnace
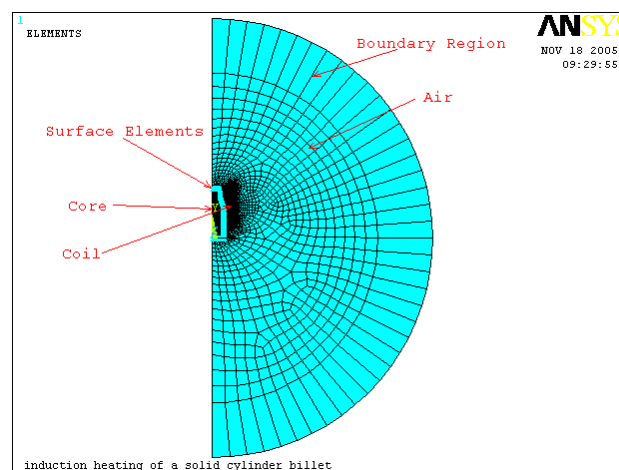and the boundary region**

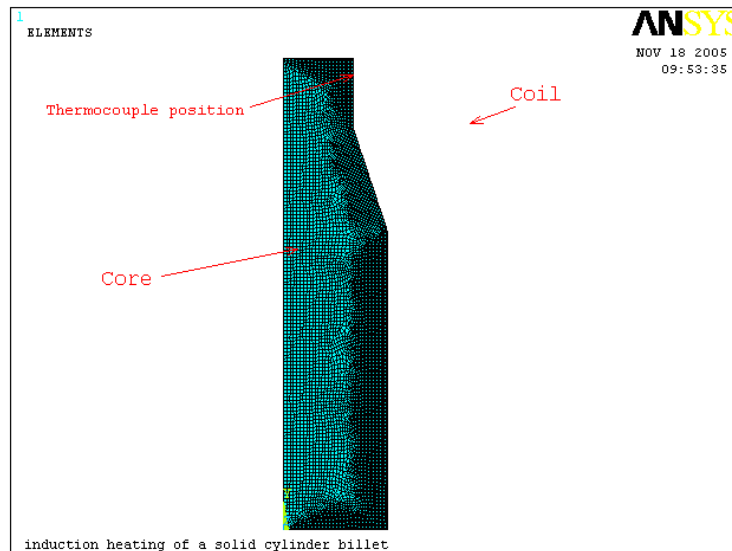**Figure (8) Shows the mesh of the boundary and the air regions**

Figure (9) The work piece mesh prepared to have higher density behind the external surfaces in order to achieve more accurate results
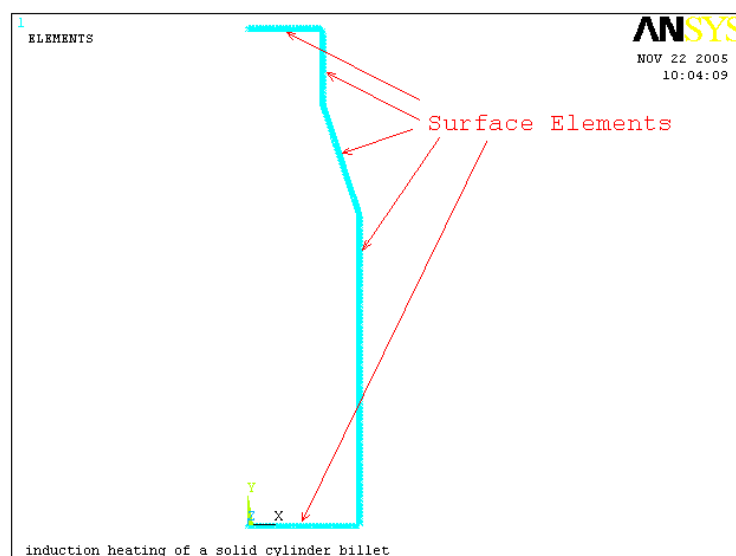

Figure (10) the positions of the surface elements surrounding the work piece

In step 4 the harmonic electromagnetic analysis is done taking into consideration the material properties for each element in the core due to its temperature, then the heat generation HGEN in Joule per unit volume and the temperature for each element fed to step 5, the transient thermal analysis part. This step needs the enthalpy and the thermal conductivity of the core material as a function of temperature $Enth(T), \lambda(T)$ as a look-up table in order to determine the temperature in degree Celsius of each element inside the core at the end of that time step. If the required value of temperature at a certain region or point in the core is reached then the program is terminated and the results are extracted as shown later on.

5. The Obtained Results

The analysis shows results describing the increase in heat at each node inside the work piece. The heating behavior of a special node number (325) at the surface is described in **Fig.(11)**. This node represents the position of the welded thermocouple of the practical measurement set declared in **Figs.(2)**, and **(9)**. The difference between the theoretical and practical curves is acceptable due to the main differences between the actual and theoretical model as it has been described. **Figure (12)** represents the heat distribution at the end of the heating time inside the work piece calculated by the theoretical computer simulation model.
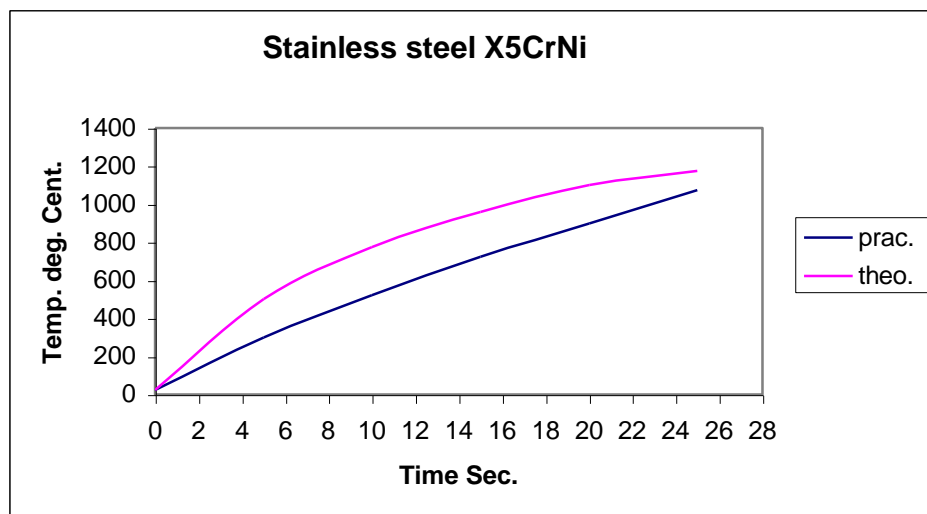

Figure (11) Temperature increase during the heating cycle for the theoretical and practical case
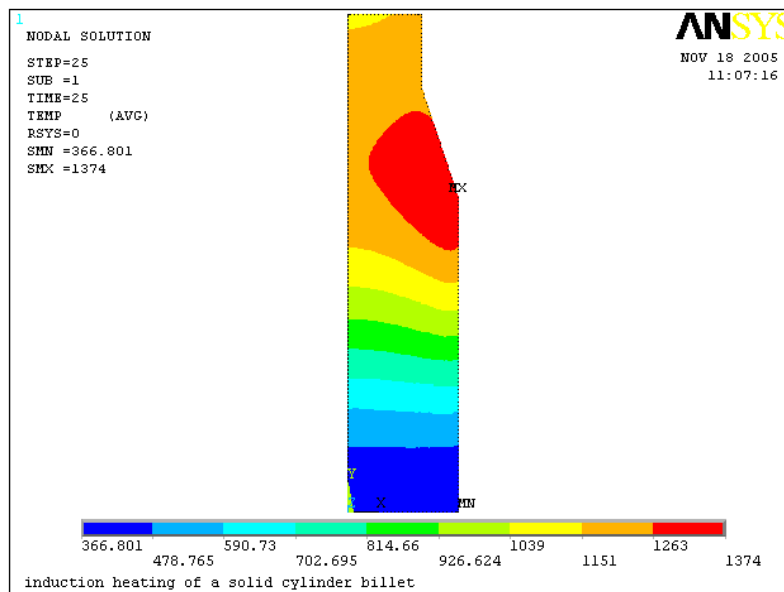

Figure (12) The heat distribution inside the work piece

6. Discussion of the Results

The calculation of this model is done for each 0.1 second during the heating period in order to achieve the most accurate results. They show a good agreement with the practical one. The slight increase in temperature between the practical and the theoretical one can be explained due to the following points:

a) In the electromagnetic model the excitation coil is considered as a single turn of solid copper plate of a cross-sectional area equal to that of the main coil, supplied by a constant current density equal to that supplied to the actual coil. The air gap between coil turns of the actual coil leads to magnetic field losses through the extremities of the coil and through the winding gaps, which are not taken into account in the model. "Another cause of discrepancy is the fact that we model a helical coil by an axi-symmetric geometry, which is an idealization of the reality." [3]. So, this may give an explanation about the slight increase of the theoretical temperature calculations on that of the practical measurements.

b) In the thermal model the coil and its lining is neglected for simplicity, so the effect of the cooling water inside the coil winding and the absorption of the heat by the lining are neglected and this may add a factor of error to the analysis.

c) The dependence functions of the physical properties ($\sigma, \rho, C_p, \lambda$) on the temperature. "Whereas the form of this dependence is generally well-known for simple bodies, this is not the case for alloys, such as different kinds of steel. Moreover, a slight variation in the composition of the alloy may have a strong influence on the physical properties. Nevertheless, simulations performed with data that approximate even in a rough way the thermal behavior of the materials give satisfactory results" [3].

d) "In this experiment, the difference between the experimental curve and the simulation during the first 10 s can be explained by the fact that the voltage cannot be set as a perfect step function." [3], hence the assumption of a constant current density along the whole period will be a source of error. Also, in such type of analysis, the temperature calculation is an accumulative process, since the temperature value at the end of any step will be considered as an initial condition for the following step, so the error in any step of calculation will be transferred to all steps following it, and it will be added to whole next points on the curve.

e) Reference 3 mention in his discussion many sources of error in the practical measurement like "The precision of the temperature measurements depends on several factors, such as the thermo-elements themselves, the quality of the thermal contact between the thermo-element and the work piece, the errors of the recording device and the reading errors. In view of our experiments, it can be roughly estimated of the order of $\pm 10°$ Celsius." And "A further factor of relevance is whether the work piece is truly concentric within the coil bore, and aligned on the same axis". This uncertainty can be added to other factors, because the results are very sensitive to the air gap distance.

Then we can affirm that the results presented above are valuable, because the error between the theoretical and the practical measurements is 9.3%, this gives the ability to extend this analysis to another industrial practice.

7. References

1. J., Davies, and P., Simpson, *"Induction Heating Handbook"*, McGraw-Hill Book Company (UK), 1979.

2. A., Vasiliev, I., Pozniak, and V., Greshnov, *"Modeling and Investigation Hardening Process"*, International Scientific Colloquium, "Modeling for Electromagnetic Processing", Hannover, March (24-26), 2003.

3. C., Chaboudez, S., Clain, R., Glardon, D., Mari, J., Rappaz, and M., Swierkosz, *"Numerical Modeling in Induction Heating for Axisymmetric Geometries"*, IEEE Trans. on Magn. Vol. 33, No. 1, January 1997, pp. 739-745.

4. C., Chaboudez, S., Clain, R., Glardon, J., Rappaz, M., Swierkosz, and R., Touzani, *"Numerical Modeling of Induction Heating of Long Workpieces"*, IEEE Trans on Magn. Vol. 30, No. 6, November 1994, pp. 5028-5037.

List of Symbols

A:	Magnetic vector potential, $Wb.m^{-1}$
B:	Magnetic flux density, Tesla
C_p:	Specific heat, $kJ/kg.^oC$
E:	Induced electromotive force, Volt
H:	Magnetic field intensity, $Amp.m^{-1}$
HGEN:	Heat generation in each element, $J.m^{-1}$
I:	Current, Amp
J:	Current density, $Amp.m^{-2}$
k:	Thermal conductivity, $W/m.^oC$
$Q_{induction}$:	The Joule heat from the electromagnetic process, $J.m^{-3}$
T:	Temperature, ^oC
t:	Time, Seconds
μ:	Permeability, $Henry.m^{-1}$
α:	Film coefficient, $W.^oC^{-1}$
ε:	Permitivity, $F.m^{-1}$
ξ:	Emissivity of the surface
ρ_e:	Electrical Resistivity, $\Omega.m$
ρ_m:	Density of material, $kg.m^{-3}$
σ_e:	Electrical conductivity, $(\Omega.m)^{-1}$
σ_s:	Stefan-Boltzmann constant, $W.m^{-2}.K^{-4}$